SECOND REVISION
21st July 2016

Hydrophobicity Effects in Iron Polypyridyl Complex Electrocatalysis within Nafion Thin-Film Electrodes

Uday Pratap Azad [a], Dharmendra Kumar Yadav [a], Vellaichamy Ganesan*[a], and Frank Marken*[b]

E-mail: VG: velganesh@yahoo.com and velgan@bhu.ac.in
FM: f.marken@bath.ac.uk

[a] *Department of Chemistry, Institute of Science, Banaras Hindu University, Varanasi- 221005, India*
[b] *Department of Chemistry, University of Bath, Bath, BA2 7AY, UK*

Abstract. Four polypyridyl redox catalysts $Fe(bp)_3^{2+}$, $Fe(ph)_3^{2+}$, $Fe(dm)_3^{2+}$, and $Fe(tm)_3^{2+}$ (with bp, ph, dm, tm representing 2,2'-bipyridine, 1,10-phenanthroline, 4,4'-dimethyl-2,2'-bipyridine, 3,4,7,8-tetramethyl-1,10-phenanthroline, respectively) are investigated for electrocatalytic oxidation of three analytes (nitrite, arsenite, and isoniazid). The polypyridyl iron complex is exchanged into a Nafion film immobilized at a glassy carbon electrode, which is then immersed in 0.1 M Na_2SO_4. Cyclic voltammetry is employed for the evaluation of the mechanism and estimation of kinetic parameters. The electrocatalytic behaviour going from low to high substrate concentration is consistent with the Albery-Hillman cases "LEty" switching to "LEk" (changing from first order in substrate to half order in substrate), which is denoting a process that occurs in a reaction zone close to the electrode surface with diffusion of charge (from the electrode surface into the film) and of anionic or neutral analyte (from the Nafion-solution interface into the film). The relative hydrophobicity of the iron polypyridyl catalyst within the film is shown to affect both the diffusion of charge/electrons and analyte within the film with $Fe(tm)_3^{2+}$ providing the mildest catalyst. All three analytes, nitrite, isoniazid, and arsenite exhibit linear calibration ranges beneficial for analytical application in a micro-molar to milli-molar range.

Keywords: electrocatalysis • Nafion • hydrophobicity effect • nitrite • arsenite • isoniazid • sensor

Graphical Abstract:

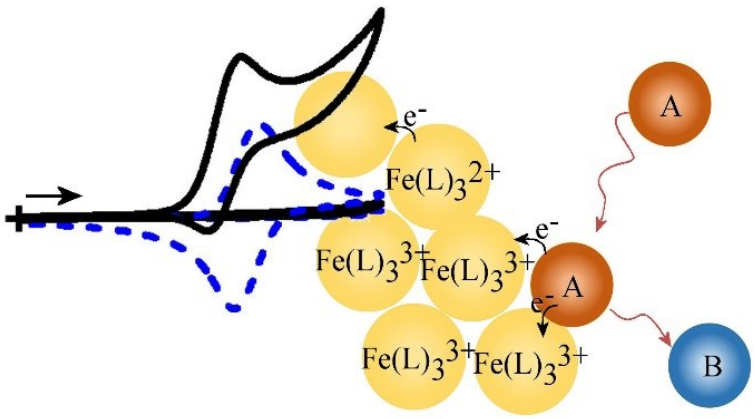

1. Introduction

Electrochemistry with metal complexes immobilised in Nafion poly-electrolyte film electrodes has been an active field of research with applications mainly in electroanalysis[1,2,3,4,5] and in fuel cell electrocatalysis.[6] A much wider field of research is that of Nafion composite film electrodes, which often provide superior analytical performance with embedded nano-oxide structures or nano-carbons.[7] Nafion is known to provide a self-assembled "channel structure" that allows proton/cation transport in hydrophilic channels surrounded by a hydrophobic polymer backbone regions.[8,9] The channel regions are lined with anionic sulfonate groups that allow permanent uptake and immobilisation of hydrophobic cations as guest molecules.[10] At the same time strong anion rejection effects have been observed.[11] It has recently been noted that this anion rejection can be overcome for the case of multiply-charged catalyst cations immobilised in the Nafion host in high concentration. In this case anions can gain access and react within the Nafion composite layer.[12,13] Nafon films are commonly employed to immobilise redox catalysts at electrode surfaces. For example, composites of cobalt porphyrin complexes and Nafion have been investigated for oxygen reduction catalysis.[14] Applications of Nafion – catalyst composites have also been suggested for organic solvent media.[15]

Multi-electron redox conversions are crucial and challenging, for example for the reduction of oxygen[16] or for the oxidation of water.[17] In order to achieve a rapid sequential transfer of electrons multiple redox centres have to work together in multi-nuclear complexes exemplified by the natural water oxidation catalyst in photosystem II based on four coupled manganese centres.[18] Oxygen reduction via a four-electron mechanism occurs in nature, for example in tetra-copper laccases,[19] and the underlying principle has been mimicked, for example with a synthetic tetra-ruthenated cobalt porphyrin oxygen reduction catalysts.[20] Multi-centre-redox systems based on tetra-ruthenated porphyrins in Nafion have also been shown to be active for multi-electron nitrite reduction.[21] Here, we suggest that hydrophobic redox centres within the channels of the Nafion host may result in a similar effect that allows multi-electron transfer reactions to proceed effectively due to high

concentration of redox centres and hydrophobicity both allowing effective multi-electron conversion. Three types of 2-electron reduction analytes are investigated: nitrite, isoniazid, and arsenite.

Isoniazid (undergoing an initial 2-electron oxidation via hydrazide intermediate[22]) is a primary and effective bacteriostatic drug for the prevention and treatment of tuberculosis.[23,24] Nitrite (oxidised to nitrate) and arsenite (oxidised to arsenate) are common and important water pollutants.[25,26] When these pollutants exceed the permissible level, they may become detrimental to human beings and/or aquatic life. Various methods/techniques have been adopted to detect/sense these pollutants/drug.[27,28,29,30,31] However, electrochemical methods offer useful alternatives to determine the same, often faster, more sensitive and in less time. The direct determination of pollutants/drugs at bare electrode surfaces generally suffers from slow electron transfer kinetics, large overpotential, low sensitivity and electrode fouling problems. To improve the sensitivity in the determination of the analyte, the operating potential should be lowered (by catalysis) as well as redox current increased (by accumulation and catalysis), which can be achieved by immobilizing suitable electrocatalysts into thin film electrodes. Various types of metal complexes, polymeric films, and enzymes[32,33,34,35,36,37,38,39,40] have been used for the modification of the electrode surface and subsequent determination of the target analytes.

It is of interest to correlate and tune the hydrophobicity of the redox catalyst embedded in the Nafion film to achieve improved analytical parameters. Here, four redox catalysts are immobilised, $Fe(bp)_3^{2+}$, $Fe(ph)_3^{2+}$, $Fe(dm)_3^{2+}$, and $Fe(tm)_3^{2+}$ (where bp, ph, dm, tm represent 2,2'-bipyridine, 1,10-phenanthroline, 4,4'-dimethyl-2,2'-bipyridine, 3,4,7,8-tetramethyl-1,10-phenanthroline, respectively; see Fig. 1). Molecules possessing more hydrophobic nature are expected to interact/aggregate more within Nafion films, influence the electrochemical properties, and consequently analytical features such as detection limit, sensitivity, and linear calibration range. Such studies are rarely attempted.[41,42,43] Some previous reports suggested a correlation of hydrophobicity with reactivity.[44,45] In this work, the immobilization of iron polypyridyl complexes are achieved following a previously published procedure.[12,39,46,47] Depending upon the metal complex immobilized in the

Nafion (Nf) thin film electrode, the resulting electrochemical systems are represented as GC/Nf/Fe(bp)$_3^{2+}$, GC/Nf/Fe(ph)$_3^{2+}$, GC/Nf/Fe(dm)$_3^{2+}$, and GC/Nf/Fe(tm)$_3^{2+}$.

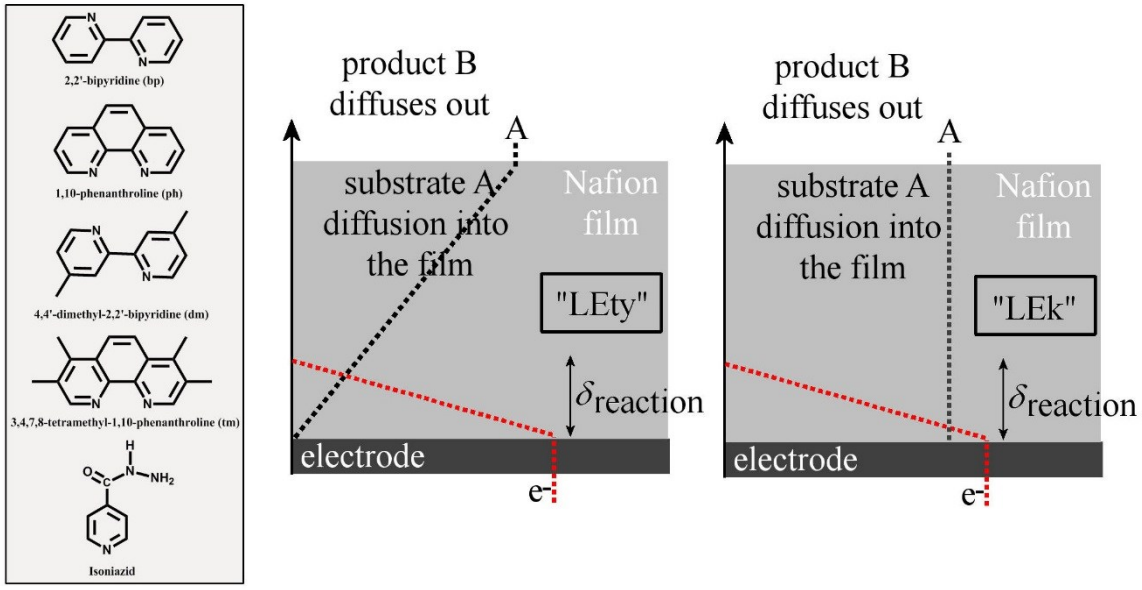

Fig. 1 Structures for ligands and isoniazid. Scheme of the reaction profile within a catalyst - Nafion composite film assuming accumulation and rapid diffusion of analyte A (black dashed line) and a "reaction layer" (red dashed line) close to the surface of the electrode. For the LEty case diffusion of reagent A is limiting (giving rise to first order kinetics) and for the LEk case the concentration of A is so high that only the bimolecular reaction at the electrode surface is rate limiting (giving rise to half order kinetics).

For the reaction mechanism based on iron polypyridyl complexes in the Nafion film two limiting cases are distinguished (see Figure 1): (i) the case of analyte film diffusion limitation ("LEty" mechanism) where the analyte concentration in the film changes linearly from the electrolyte|Nafion interface to the Nafion|electrode interface and (ii) the case of kinetic rate limitation ("LEk" mechanism) where transport of analyte is fast and the concentration essentially constant across the Nafion film. When changing the concentration of analyte A in the electrolyte solution, it is possible to switch from LEty to LEk which is associated with a characteristic change in the voltammetric response.

2. Experimental section

2.1 Chemicals. Nafion (5 wt% solution in lower aliphatic alcohols), 2,2'-bipyridine (bp), 4,4'-dimethyl-2,2'-bipyridine (dm), 1,10-phenanthroline (ph), 3,4,7,8-tetramethyl-1,10-phenanthroline (tm), and sodium arsenite ($NaAsO_2$) were purchased from Aldrich. Sodium sulfate, sodium nitrite, isoniazid (IZ), and ferrous ammonium sulfate were purchased from S.D. Fine or SRL, India. Sulfates of tris(2,2'-bipyridine) iron(II) ($Fe(bp)_3^{2+}$), tris(4,4'-dimethyl-2,2'-bipyridyl) iron(II) ($Fe(dm)_3^{2+}$), tris(1,10-phenanthroline) iron(II) ($Fe(ph)_3^{2+}$), and tris(3,4,7,8-tetramethyl-1,10-phenanthroline) iron(II) ($Fe(tm)_3^{2+}$) were prepared and characterized according to reported literature procedures.[48,49,50] All other chemicals were of analytical-reagent grade and were used without further purification. Triply distilled water was used in all the experiments.

2.2 Instrumentation. Electrochemical experiments were performed with CHI 660C (CH Instruments, USA) electrochemical workstation using a three-electrode configuration. Bare or modified glassy carbon electrodes (GC, 0.07 cm^2 area) were used as working electrodes, platinum wire was used as counter electrode, and an Ag/AgCl (saturated KCl) was used as reference electrode. Thus, in this study the potentials are referred to Ag/AgCl electrodes unless otherwise mentioned. For UV-Vis spectral measurements of metal complexes in Nafion films on clean glass plates of 1.0 cm^2 area were used. The thickness of the Nafion film was maintained (ca. 0.9 μm) in all experiments. A 2802 PC UV-Vis spectrophotometer (Unico, USA) was used to measure the UV-Vis absorbance spectra. All electrochemical experiments were carried out at room temperature (25 ± 2 ºC). Before each electrochemical measurement, solutions were purged with nitrogen.

2.3 Electrode preparation. Glassy carbon (GC) electrode surfaces were polished with 0.05 μm alumina powder on a wet polishing cloth. The polished electrodes were sonicated in an ultrasonic cleaner for 5 min and then rinsed with distilled water several times. Nafion coated GC electrodes (GC/Nf) (typical thickness 0.9 μm) were prepared following the procedure used in previous reports.[12,39,46,47] GC/Nf/$Fe(bp)_3^{2+}$, GC/Nf/$Fe(dm)_3^{2+}$, GC/Nf/$Fe(ph)_3^{2+}$, and GC/Nf/$Fe(tm)_3^{2+}$ electrodes were prepared by dipping GC/Nf electrodes in 0.5 mM aqueous solutions of respective metal complexes for 30 min and then

rinsing with triple distilled water. Metal complex ions were exchanged/immobilized onto electrodes and were then continuously potential cycled between 0.2 to 1.3 V vs. Ag/AgCl in 0.1 M Na_2SO_4 (scan rate 20 mVs^{-1}) until a constant current was observed. The amount of FeL_3^{2+} incorporated into Nafion film was estimated from the difference in absorbance before and after dipping the electrode in 0.5 mM solution of the corresponding FeL_3^{2+} complex.

2.4 Calculation of percentage of increasing oxidation current. The percentage of increase in oxidation current was calculated based on the equation *Percentage of increasing oxidation current* = $[(I_{pa}-I_{pa,0})/I_{pa,0}] \times 100$. Here $I_{pa,0}$ represents the anodic peak oxidation current in the absence of analyte/substrate and I_{pa} represents the anodic peak oxidation current in the presence of analyte.

3. Results and discussion

3.1 Spectral characteristics of iron polypyridyl complexes in Nafion film

Metal complex exchanged Nafion films on a glass plate show absorption maxima at 524, 512, 528 and 504 nm for $Fe(bp)_3^{2+}$, $Fe(ph)_3^{2+}$, $Fe(dm)_3^{2+}$ and $Fe(tm)_3^{2+}$ (curve a in Fig. 2A, 2B, 2C, and 2D, respectively) indicating the immobilization of the respective metal complexes "intact" into the Nafion film. Aqueous solutions of corresponding metal complexes show absorption maxima at 522, 510, 529, and 500 nm (curve a' in Fig. 2A, 2B, 2C, and 2D, respectively). No significant change in the peak positions was observed after being incorporated into Nafion[51] signifying that the immobilized metal complexes are viable to be utilized for further studies. The UV/Vis absorption data were employed to estimate the concentration of redox active iron polypyridyl complexes in Nafion (see Table 1).

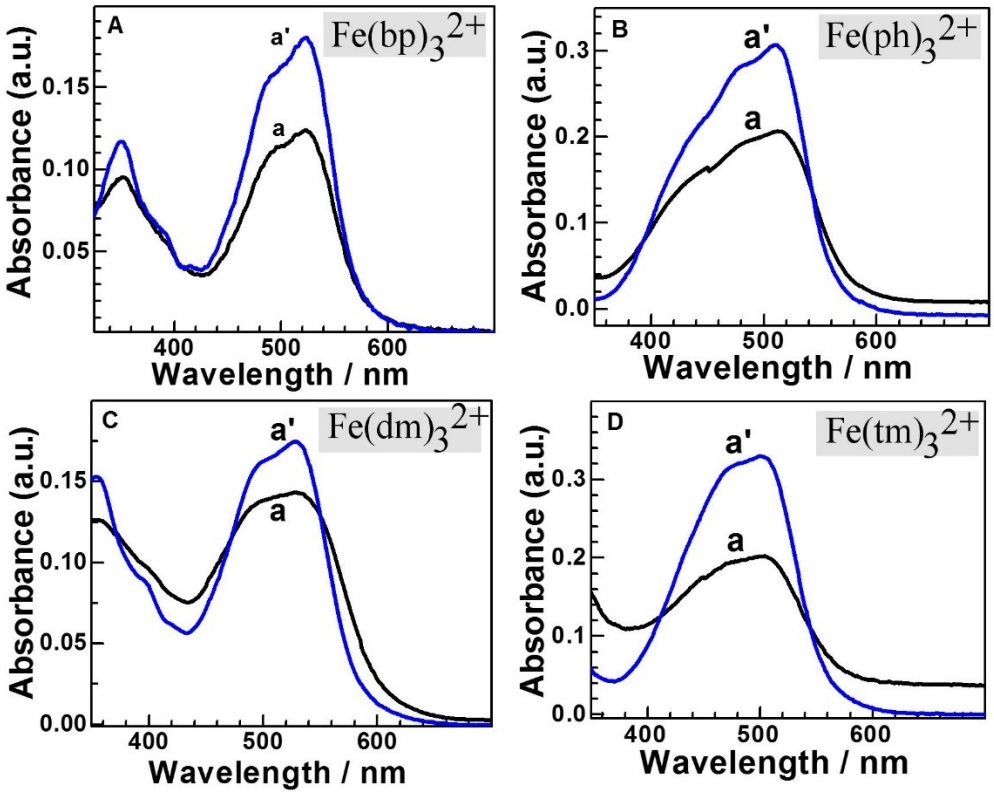

Fig. 2 UV-Vis absorption spectra of (A) $Fe(bp)_3^{2+}$, (B) $Fe(ph)_3^{2+}$, (C) $Fe(dm)_3^{2+}$, and (D) $Fe(tm)_3^{2+}$ immobilized into Nafion on a glass plate (a) and in aqueous solution (a').

3.2 Electrochemical characteristics of iron polypyridyl complexes in Nafion films

Cyclic voltammograms of the four immobilized iron polypyridyl complexes, GC/Nf/$Fe(bp)_3^{2+}$, GC/Nf/$Fe(ph)_3^{2+}$, GC/Nf/$Fe(dm)_3^{2+}$, and GC/Nf/$Fe(tm)_3^{2+}$ immersed in 0.1 M Na_2SO_4 as a function of scan rate are shown in Fig. 3 (A, B, C, and D, respectively).

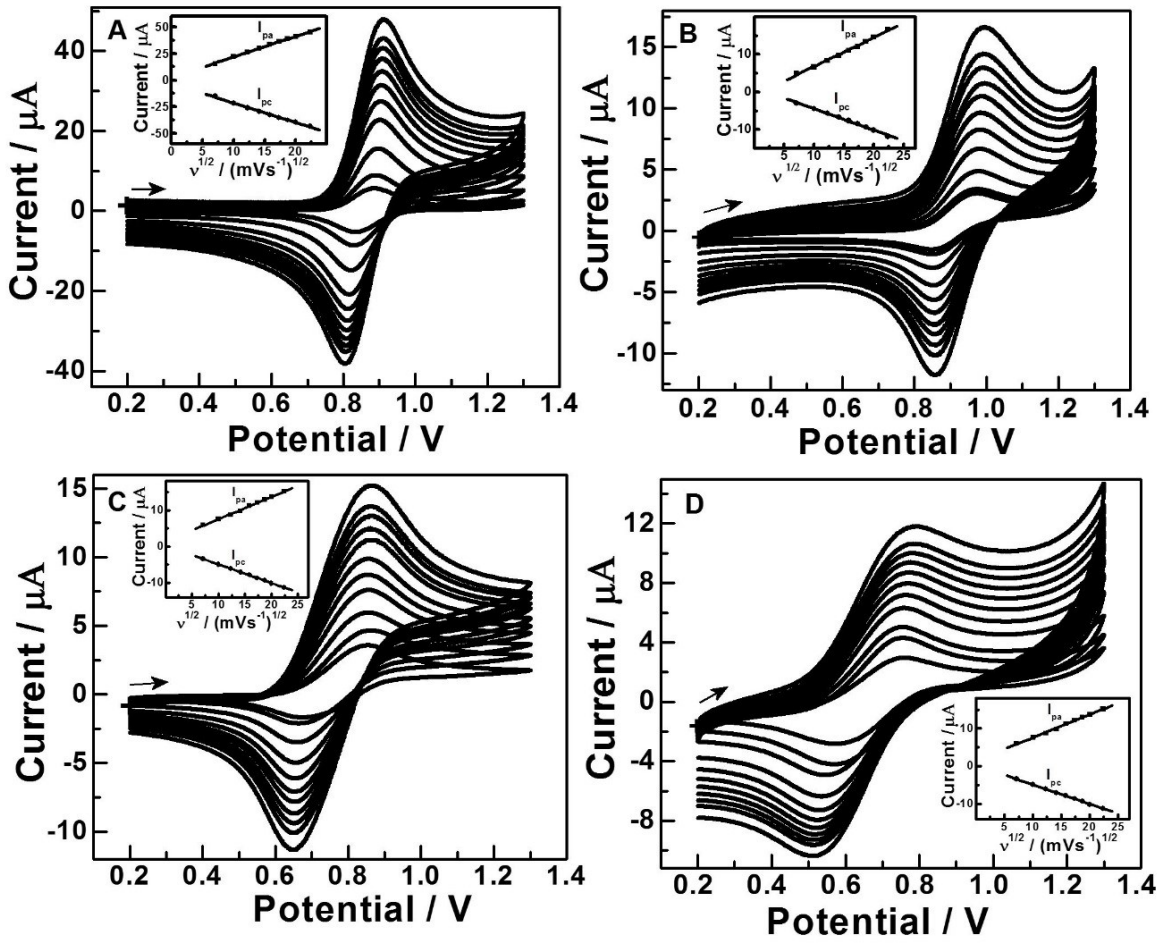

Fig. 3 Cyclic voltammograms (scan rate 10, 20, 50, 100, 200, 250, 300, 350, 400, 500 mV s^{-1}) for (A) GC/Nf/Fe(bp)$_3^{2+}$, (B) GC/Nf/Fe(ph)$_3^{2+}$, (C) GC/Nf/Fe(dm)$_3^{2+}$, and (D) GC/Nf/Fe(tm)$_3^{2+}$ electrodes immersed in 0.1 M Na_2SO_4. Insets show linear dependences of peak currents I_{pa} and I_{pc} plotted *versus* the square root of scan rate.

Well-defined oxidation and reduction peaks are observed, which can be attributed to one-electron $FeL_3^{2+/3+}$ redox processes. Table 1 summarizes the $E_{1/2} = ½(E_{pa} + E_{pc})$ values together with other electrochemical parameters of the modified electrodes. The observed $E_{1/2}$ values for different metal complexes are consistent with previously reported values[52] and show a similar hydrophobicity-dependent trend in both the Nafion film environment and in aqueous solution. Fe(tm)$_3^{2+}$ appears to be oxidised at a potential approximately 0.2 V more negative compared to Fe(bp)$_3^{2+}$. Generally, a small negative shift in $E_{1/2}$ when going from aqueous solution to Nafion environment suggests stabilisation of the more

cationic Fe(III) polypyridyl complex in the Nafion environment with $Fe(tm)_3^{2+}$ exhibiting the biggest shift (80 mV) possibly linked to a more hydrophobic character or a change in anion binding.

Table 1 Electrochemical parameters for iron polypyridyl complex modified glassy carbon electrodes in 0.1 M Na_2SO_4 (scan rate = 20 mVs^{-1}).

Electrode	**$E_{1/2}$ ($E_{1/2,free}$) [a] /V vs. Ag/AgCl**	**I_{pa}/I_{pc}**	**ΔE_p =(E_{pa}-E_{pc}) /mV**	**C_{cat} [b] / mol m^{-3}**	**D_{app} [c] /10^{-14} m^2 s^{-1}**
GC/Nf/$Fe(bp)_3^{2+}$	0.86 (0.91)	1.0 ± 0.1	60	120	9.3
GC/Nf/$Fe(ph)_3^{2+}$	0.93 (0.94)	1.0 ± 0.1	108	86	2.2
GC/Nf/$Fe(dm)_3^{2+}$	0.73 (0.78)	1.0 ± 0.1	157	57	3.9
GC/Nf/$Fe(tm)_3^{2+}$	0.64 (0.72)	1.0 ± 0.1	170	42	3.1

[a] $E_{½} = ½ (E_{p,a} + E_{p,c})$; $E_{½,free}$ obtained for 1 mM FeL_3^{2+} dissolved in aqueous 0.1 M Na_2SO_4.
[b] estimated from UV/Vis adsorption data; estimated error ± 20%; an additional error may arise from some adsorbed iron polypyridyl complex not being redox active.
[c] obtained from cyclic voltammetry data in aqueous 0.1 M Na_2SO_4; error ± 40% mainly due to error in concentration C_{cat}.

The observed peak current at the modified electrodes follow the trend $Fe(bp)_3^{2+} > Fe(ph)_3^{2+} \approx Fe(dm)_3^{2+} > Fe(tm)_3^{2+}$, which is just opposite to the hydrophobicity sequence of the redox catalyst. The trend in peak currents is at least approximately consistent with the concentration estimates for iron polypyridyl complexes within the Nafion film (Table 1)), but may also be further affected by changes in the rate of inter-molecular electron transfer in Dahms-Ruff diffusion. Cyclic voltammetry data was analysed to extract apparent charge diffusion rate information (employing the Randles-Sevcik equation[53]) and the corresponding apparent diffusion coefficient D_{app} values (see Table 1). These values reflect charge mobility and are likely to be associated at least in part with Dahms-Ruff charge

hopping.[54,55] A decrease in charge mobility appears to be weakly correlated to an increase in hydrophobicity (with the exception of $Fe(ph)_3^{2+}$). This trend can be understood in terms of loss of mobility of the more hydrophobic metal complex in the Nafion host matrix causing less effective collisional hopping of charges.[56] The magnitude of the D_{app} values is consistent with relatively slow diffusion within the film in all cases. On increasing the hydrophobicity of the redox active complex, the peak-to-peak separation (ΔE_p) seems increased, possibly indicating a less reversible electron transfer at the electrode | Nafion film interface or some association of the iron polypyridyl complex with counter anions in particular for the more hydrophobic catalysts (leading to more "square scheme-like" reactivity[57]). It is interesting to compare the reversible potentials for $FeL_3^{2+/3+}$ in solution with the corresponding reversible potentials when immobilised in Nafion (Table 1). The oxidised species (*i.e.* FeL_3^{3+}) seem slightly stabilized in Nafion films (potentials shift negative by 10 to 80 mV), presumably due to the increase in the anion availability in Nafion. The highest shift is observed for $Fe(tm)_3^{2+/3+}$ possibly due to increased hydrophobicity causing stronger interactions with anions relative to those with water.

3.3 Electrocatalytic oxidation of anionic analytes

Fig. 4 shows cyclic voltammetry data for the oxidation process of the three analytes at different metal complex modified electrodes, GC/Nf/FeL_3^{2+}, together with data for the unmodified (GC/Nf) electrode. Cyclic voltammograms for the unmodified electrode did not show any peaks in the potential range 0.2 to 1.3 V vs. Ag/AgCl in 0.1 M Na_2SO_4 (see a in Fig. 4A-C). However, nitrite and isoniazid can be irreversibly oxidized at the bare electrode with oxidation peak potentials at 1.19 and 1.01 V vs. Ag/AgCl (see a' in Fig. 4A and B). Arsenite is not oxidized at the bare electrode (see a' in Fig. 4C). With iron polypyridyl catalysts all the three analytes are oxidized at less positive potentials (see b' in Fig. 4A-C). As tell-tale sign for electrocatalysis during the positive going potential scan, enhanced anodic currents are observed whereas during the negative going potential scan no cathodic current is observed.

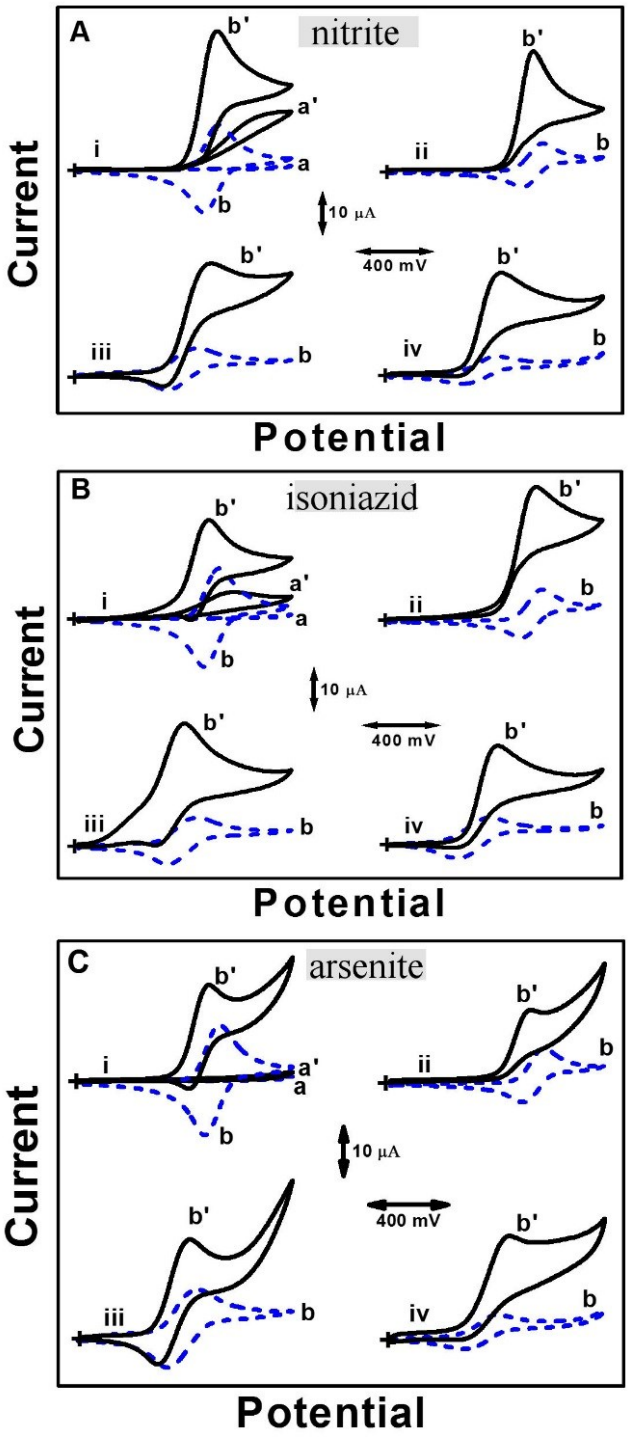

Fig. 4 Cyclic voltammograms (scan rate 20 mVs^{-1}) for the electrocatalytic oxidation of (A) nitrite, (B) isoniazid, and (C) arsenite at (i) GC/Nf (a,a') and GC/Nf/Fe(bp)$^{2+}$ (b,b'), (ii) GC/Nf/Fe(ph)$^{2+}$ (b,b'), (iii) GC/Nf/Fe(dm)$^{2+}$ (b,b'), and (iv) GC/Nf/Fe(tm)$^{2+}$ (b,b') electrodes immersed in 0.1 M Na_2SO_4 in the absence (a, b) and presence (a', b') of 1.0 mM of the respective analytes.

The electrocatalytic shift in oxidation potentials and percentage of increasing oxidation current (see Experimental) can be calculated. Data for the nitrite, isoniazid, and arsenite oxidations at the FeL_3^{2+} immobilized electrodes are summarised in Table 2.

Table 2 Oxidation peak potentials and the percentage of increasing oxidation current of analytes at GC/Nf/FeL_3^{2+} electrodes.

Analyte	Oxidation peak potentials (V vs. Ag/AgCl) and in brackets % of increase in the oxidation current at GC/Nf/FeL_3^{2+} electrodes for 1 mM analyte at scan rate 20 mVs^{-1}.			
	$Fe(bp)_3^{2+}$	$Fe(ph)_3^{2+}$	$Fe(dm)_3^{2+}$	$Fe(tm)_3^{2+}$
Nitrite	0.92 (210)	0.94 (334)	0.89 (340)	0.77 (489)
Isoniazid	0.87 (99)	0.90 (340)	0.75 (330)	0.74 (408)
Arsenite	0.86 (64)	0.90 (116)	0.78 (206)	0.77 (361)

It is noteworthy that $Fe(tm)_3^{2+}$ electrocatalytically oxidize all the three analytes at significantly less positive potentials. In spite of this, the percentage of increase in oxidation peak current at GC/Nf/$Fe(tm)_3^{2+}$ is always higher than those observed for other iron polypyridyl complexes. This is probably linked to the lower current in the absence of analyte causing a bigger relative change. The large increase in current in the presence of analytes can be used for the more sensitive analytical determination (*vide infra*). In our earlier report[12] it was highlighted that when Nafion film is fully exchanged with cationic metal complex, the uptake and diffusion of anionic species (such as nitrite) can be enhanced and therefore the negatively charged analytical species can be determined at the cation exchange polymer (where usually anion rejection effects would dominate). A schematic illustration of the proposed catalytic processes for the oxidation of anionic analytes (contrasting mechanistic cases for low and at high analyte concentration) within the Nafion film is shown in Fig. 1.

Further evidence for the catalytic nature of the reaction occurring within the Nafion layer, which is consistent with the case of charge transport from the electrode surface competing

either with transport of analyte or with the catalytic reaction (these are the Albery-Hillman cases "LEty" and "LEk", respectively[58]), can be obtained from analysis of cyclic voltammetry experiments. Data from cyclic voltammetry in the presence of analyte are shown in Fig. 5. The increase in the catalytic current I_{cat} with analyte can be interpreted in terms of the reaction rate increasing and corresponding the reaction layer thinning.

In order to quantify the reaction rate without any knowledge of the analyte concentration $C_{analyte,Nafion}$ or the diffusion coefficient for the analyte $D_{analyte,Nafion}$ within the Nafion film, it is possible to evaluate the reaction layer thickness $\delta_{reaction}$ (see scheme in Fig. 1) as a measure of reactivity. This is attempted here in the limit of high analyte concentration (here at 100 mM concentration) in order to explore the limit of reactivity in terms of the reaction layer thickness. Equation 1 is employed to express the case of the catalytic current, I_{cat} (see Fig. 5), as given by the Faraday constant F, the electrode area A, the apparent diffusion rate of charges D_{app} (see Table 1), and the concentration of catalyst C_{cat} (see Table 1). The reaction layer thickness $\delta_{reaction}$ can be estimated (see Table 3) using equation 1.

$$I_{cat} = \frac{F\ A\ D_{app}\ C_{cat}}{\delta_{reaction}} \qquad (1)$$

Values for the reaction layer thickness vary from 2.6 nm to 47 nm, which in all cases is consistent with a reaction close to the electrode surface. Comparison of the 4 catalyst systems suggests insignificant changes and therefore $Fe(tm)_3^{2+}$ being just as efficient as the other catalysts. Arsenite can be seen to be associated with the most extended reaction layer consistent with a "difficult" or relatively slow multi-electron catalytic reaction. Nitrite appears to react fast (= thin reaction layer) in particular for the more hydrophobic catalyst systems. Isoniazid also reacts faster in the presence of the more hydrophobic catalysts. Note that both nitrite and isoniazid also exhibit direct electron transfer in addition to the electrocatalytic reaction (see Fig. 4).

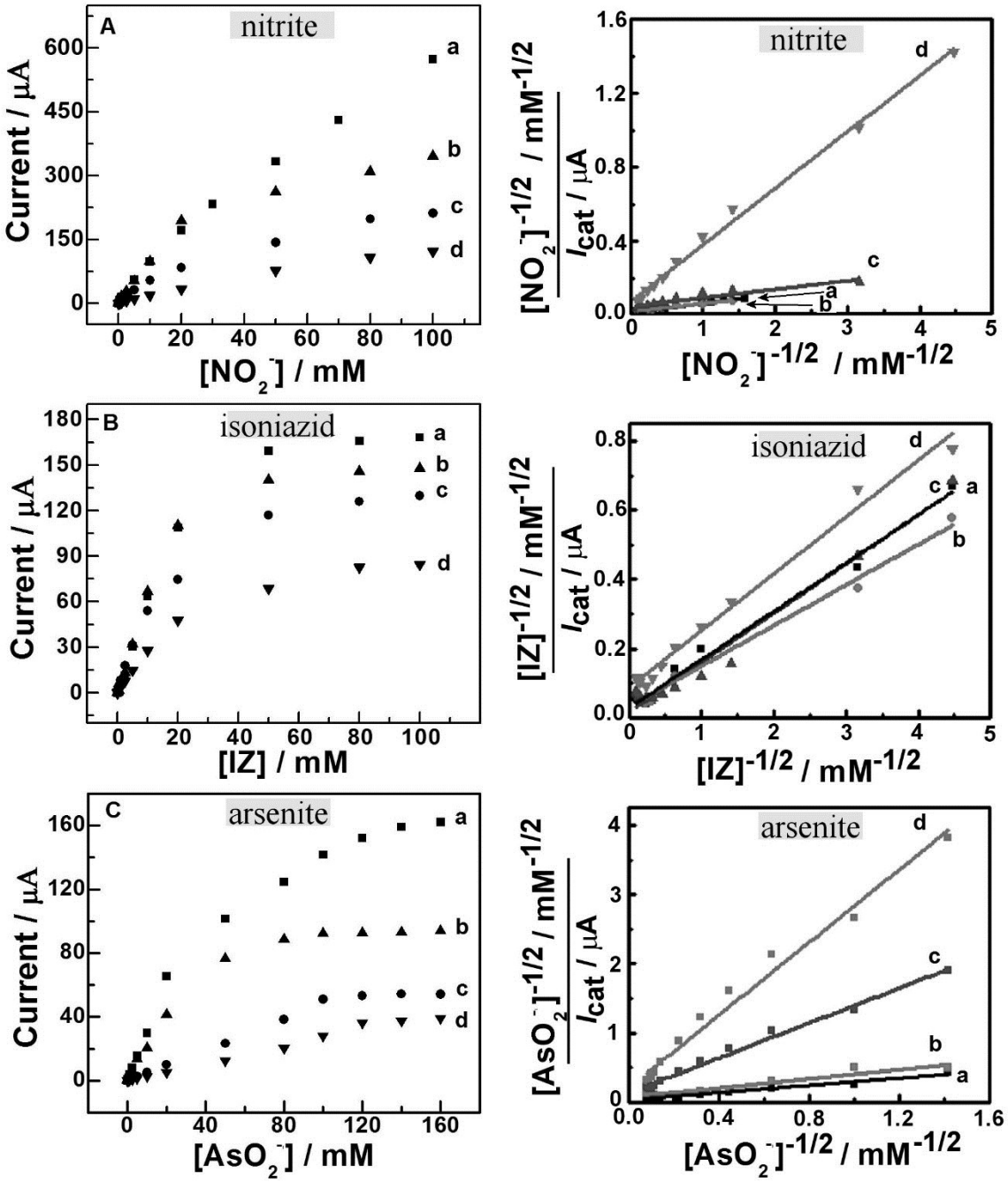

Fig. 5 Variation of anodic catalytic oxidation currents (based on cyclic voltammograms with scan rate 20 mV s^{-1}) with different concentrations of analytes. (A) Nitrite, (B) isoniazid, and (C) arsenite at (a) GC/Nf/Fe$(bp)_3^{2+}$, (b) GC/Nf/Fe$(ph)_3^{2+}$, (c) GC/Nf/Fe$(dm)_3^{2+}$, and (d) GC/Nf/Fe$(tm)_3^{2+}$ electrodes. Also shown are plots of square root analyte concentration over catalytic current versus square root of analyte concentration as evidence for LEty to LEk mechanistic transition (see text).

Table 3 Limiting reaction layer based on increasing oxidation current with analytes at GC/Nf/FeL_3^{2+} electrodes (scan rate 20 mVs^{-1}).

Analyte	Reaction layer thickness data $\delta_{reaction}$ obtained from the oxidation current at GC/Nf/FeL_3^{2+} electrodes for 100 mM analyte.			
	$Fe(bp)_3^{2+}$	$Fe(ph)_3^{2+}$	$Fe(dm)_3^{2+}$	$Fe(tm)_3^{2+}$
Nitrite	12 nm	2.6 nm	6.5 nm	5.9 nm
Isoniazid	42 nm	6.6 nm	11 nm	11 nm
Arsenite	47 nm	9.9 nm	25 nm	22 nm

Although current data obtained with cyclic voltammetry are transient in character and not strictly in the pure kinetic domain (for this usually rotating disk voltammetry with extrapolation to infinitely high rotation rates is applied[59]), it can be suggested that in particular at lower scan rates and at higher analyte concentration mass transport effects from outside the Nafion film diminish and expressions derived for the steady state limiting case can be used at least in first approximation. When expressing the current as $I_{peak} = AF[\text{analyte}]k_{EC}$ (with A the area, F the Faraday constant, and k_{EC} the electrochemical rate constant) and when combining the rate constant expressions for "LEty" and "LEk" cases with $k_{EC,LETy} = KD_{analyte,Nafion}/L$ and $k_{EC,LEk} = KC_{cat}(kD_{app}/[\text{analyte}])^{0.5}$ (with L the thickness of the Nafion layer and K the analyte partitioning constant between aqueous phase and Nafion), expression 2 is obtained, which suggests a transition in the current versus analyte concentration dependence going from first order to half order.

$$I_{peak} = \frac{a[analyte]}{b+\sqrt{[analyte]}} \qquad (2)$$

with $a = AFKC_{cat}\sqrt{k\,D_{app}}$; $b = \frac{L\,C_{cat}}{D_{analyte,Nafion}}\sqrt{k\,D_{app}}$; $\frac{a}{b} = \frac{A\,F\,K\,D_{analyte,Nafion}}{L}$

In this expression k is the second order rate constant for the catalytic reaction in the Nafion film. Equation 2 is readily linearised to equation 3 with the corresponding plots presented in Figure 5.

$$\frac{\sqrt{[analyte]}}{I_{peak}} = \frac{b}{a}\frac{1}{\sqrt{[analyte]}} + \frac{1}{a} \qquad (3)$$

From experimental data it appears that in all three cases of analytes reasonably linear dependencies are observed for all catalysts and at least over part of the concentration range. This confirms the proposed transition from the LEty case at lower analyte concentration to the LEk case at higher analyte concentrations. The slope b/a for $Fe(tm)_3^{2+}$ is consistently the highest, which may be an indication for $D_{analyte,Nafion}$ being the lowest (see equation 2). Note that $D_{analyte,Nafion}$ is a real diffusion coefficient in contrast to D_{app}, which is associated also with charge hopping. Also note the slope for arsenite being higher compared to that for nitrite, which is likely to be a sign of slower transport for the multiply charged anion (AsO_3^{3-}). However, further quantitative analysis of the data appears unwarranted due to the approximations made and due to the error in intercepts. The true values for the rate constant k as a function of hydrophobicity remain therefore unknown.

3.4 Electrochemical determination of analytes

To test the analytical determination of nitrite, isoniazid, and arsenite at the FeL_3^{2+} complex modified Nafion film electrodes, cyclic voltammmograms (at 20 mVs^{-1} scan rate) were recorded with different concentrations of each analyte and immersed in aqueous 0.1 M Na_2SO_4. The observed anodic currents are used to construct the calibration graphs and shown in Fig. 6.

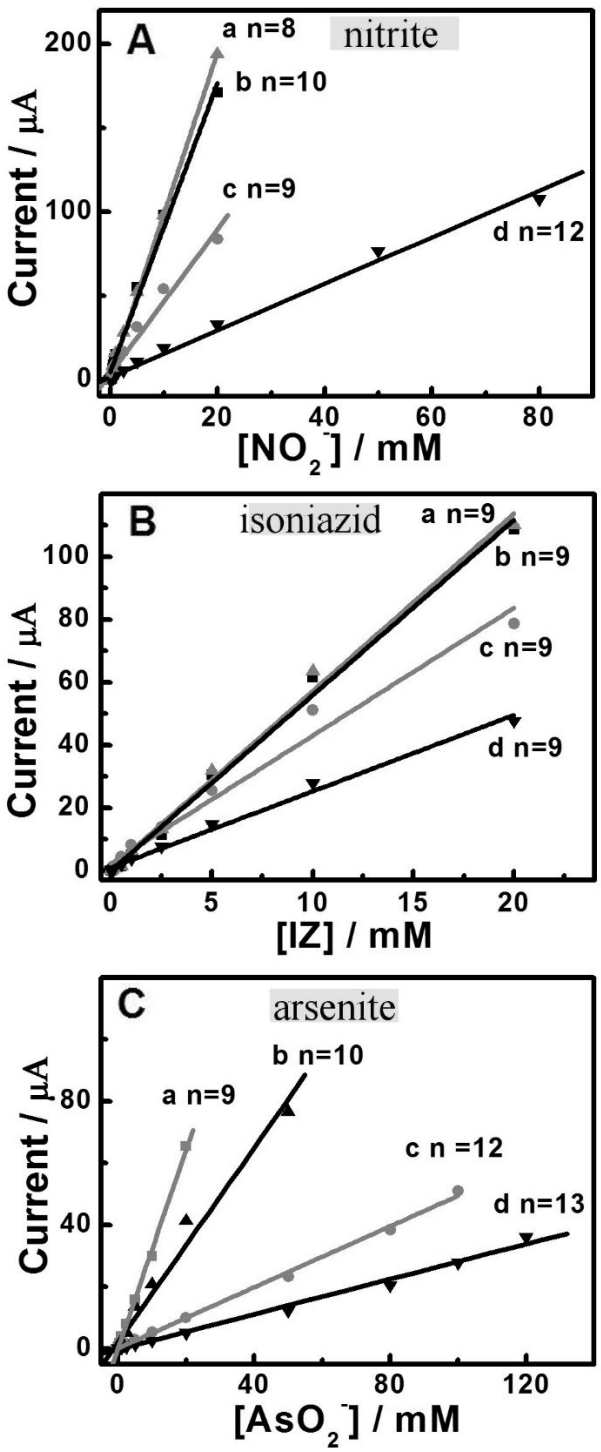

Fig. 6 Linear dependence of anodic oxidation current (from cyclic voltammograms with scan rate 20 mVs^{-1}) with successive additions of (A) nitrite, (B) isoniazid, and (C) arsenite at (a) GC/Nf/$Fe(bp)_3^{2+}$, (b) GC/Nf/$Fe(ph)_3^{2+}$, (c) GC/Nf/$Fe(dm)_3^{2+}$, and (d) GC/Nf/$Fe(tm)_3^{2+}$ electrodes immersed in 0.1 M Na_2SO_4. Here "n" represents number of additions of analyte. Note that at higher substrate concentration deviation from linearity occurs.

It is observed that concentrations of nitrite as low as 0.01 mM can cause an increase in the oxidation current (Fig. 6A). The oxidation current linearly varies over several orders of magnitude from 0.01 mM to 20 mM (at GC/Nf/Fe$(bp)_3^{2+}$, Fig. 6A-a) or up to 80 mM (at GC/Nf/Fe$(tm)_3^{2+}$, Fig. 6A-d). The other iron polypyridyl complexes (GC/Nf/Fe$(ph)_3^{2+}$ in Fig. 6A-b and GC/Nf/Fe$(dm)_3^{2+}$ in Fig. 6A-c) show linear variation in a range of 0.01 mM to 10 mM and 0.01 mM to 15 mM, respectively). These linear ranges are analytically beneficial and extended when compared to previous studies.[60,61,62,63,64,65,66,67,68,69,70] Table 4 shows the linear calibration range data for different modified electrodes together with other parameters for nitrite determination.[12] On further increasing the concentration of nitrite above the linear range, there is a deviation from linearity and the oxidation currents vary sub-linearly (as is expected for the Albery-Hillman case transition LEty to LEk). Similar results are observed for the determinations of isoniazid and the analytical parameters are summarised in Table 5.[47] The electrocatalytic oxidation of arsenite at the FeL_3^{2+} based Nafion film electrodes provide a linear variation in current with concentration as shown in Fig. 6C and Table 6.[39]

Sensor electrodes with Nafion film deposits are generally very robust against interferences. For interference studies on FeL_3^{2+} immobilized electrodes, 1.0 mM concentration of analyte is used and 50-fold excess of interfering substances is added. Experiments were performed under similar conditions as that used for the construction of the calibration graphs (cyclic voltammetry with scan rate 20 mVs^{-1} in 0.1 M Na_2SO_4). For nitrite interferences from chloride, nitrate, carbonate, acetate, Cu^{2+}, K^+, glucose, and urea remained below 6%. For arsenite effects from nitrate, Al^{3+}, dichromate, Hg^{2+}, Cd^{2+}, permangante, Ba^{2+}, Mg^{2+}, Ca^{2+}, Pb^{2+}, and Zn^{2+} on the anodic signal remained below 8%. During the electrochemical determination of isoniazid, hydrazine (the principle interferent) had no detrimental effect on the oxidation current signal.

Stability and reproducibility were examined during continuous potential cycling (between 0.2 to 1.3 V vs. Ag/AgCl). The initial decrease in current (between 1st and 20th cycles) is

5-8% and due to some leaching of FeL_3^{2+} into the supporting electrolyte solution. Between the 20th cycle to the 100th cycle typically about 2% further loss is observed. The operational stability of FeL_3^{2+} immobilized electrodes for the determination of analytes was evaluated using a single electrode (within electrode variation) and also using several (at least four) electrodes (between electrodes variation) for a particular metal complex and for a particular analyte. The relative standard deviation (RSD) for the four determinations is 8.0%. Similarly, four different electrodes of $Fe(bp)_3^{2+}$ are used for the determination of nitrite under the identical conditions to produce a RSD of 12%. The lowest RSDs are obtained at the $Fe(tm)_3^{2+}$ immobilized electrodes for the determination of arsenite as 3.8% (within electrode variation) and 5.8% (between the electrodes variation). Long term stability of these electrodes was evaluated based on their responses at regular intervals for 30-60 days. The percentage of decrease in current between the first day and 30th day is found to be 4-5% for $Fe(bp)_3^{2+}$ for the determination of nitrite. For $Fe(tm)_3^{2+}$ immobilized electrodes towards the determination of arsenite 3-4% decrease in oxidation current is observed between the first day and the 60th day. Thus the operational and long term stability of these electrodes is better for $Fe(tm)_3^{2+}$ immobilized electrodes than for the other FeL_3^{2+} immobilized electrodes and for all analytes.

Table 4 Comparison of analytical parameters for the determination of nitrite.

Method	Electrode	Medium	Oxidation potential (V)	Detection limit (µM)	Sensitivity (µA/µM)	Linear calibration range (µM)	Reference
CV	GC/Nf/Fe(bp)$_3^{2+}$	0.1 M sodium sulfate	0.92	30	0.0086	200-20000	12
CV	GC/Nf/Fe(dm)$_3^{2+}$	0.1 M sodium sulfate	0.89	10	0.0031	10-20000	Present work
CV	GC/Nf/Fe(ph)$_3^{2+}$	0.1 M sodium sulfate	0.94	10	0.48	10-20000	Present work
CV	GC/Nf/Fe(tm)$_3^{2+}$	0.1 M sodium sulfate	0.77	10	0.0083	10-80000	Present work

Table 5 Summary of analytical parameters for isoniazid determination.

Method	Electrode	Medium	Oxidation potential (V)	Detection Limit (µM)	Sensitivity (µA/µM)	Linear calibration range (µM)	Reference
CV	GC/Nf/Fe(tm)$_3^{2+}$	0.1 M sodium sulfate	0.74	13	0.0025	50 - 20000	47
CV	GC/Nf/Fe(ph)$_3^{2+}$	0.1 M sodium sulfate	0.90	10	0.0074	10-20000	Present work
CV	GC/Nf/Fe(bp)$_3^{2+}$	0.1 M sodium sulfate	0.87	10	0.031	10-20000	Present work
CV	GC/Nf/Fe(dm)$_3^{2+}$	0.1 M sodium sulfate	0.75	10	0.010	10-20000	Present work

Table 6 Comparative analysis for electrocatalytic oxidative determination of arsenite.

Method	Electrode	Medium	Oxidation potential (V)	Detection Limit (µM)	Sensitivity (µA/µM)	Linear calibration range (µM)	Reference
CV	GC/Nf/Fe(dm)$_3^{2+}$	0.1 M sodium sulfate	0.78	10	0.0021	10-100000	39
CV	GC/Nf/Fe(bp)$_3^{2+}$	0.1 M sodium sulfate	0.86	10	0.21	10-20000	Present work
CV	GC/Nf/Fe(ph)$_3^{2+}$	0.1 M sodium sulfate	0.90	10	0.0035	10-50000	Present work
CV	GC/Nf/Fe(tm)$_3^{2+}$	0.1 M sodium sulfate	0.77	10	0.0013	10-120000	Present work

4. Conclusions

When studying iron polypyridyl complex catalytic activity for oxidation of three types of analyte, the electrode GC/Nf/Fe(tm)$_3^{2+}$ showed the most negative (mild) redox potential and a high percentage of oxidation current increase in comparison to all other types electrodes. Further analysis of peak currents based on the approximate model of a transition from "LEty" case to "LEk" case confirmed consistent catalytic reactivity for all four catalysts. Hydrophobicity effects on the rate of the catalytic reaction appear insignificant (and are not fully quantified), but mobility of both charges and analyte within the Nafion film seem affected. For high levels of analyte concentration, typical reaction layer thicknesses range from 2.6 nm to 47 nm.

In case of arsenite, an unexpectedly broad linear calibration range was obtained at all types of modified electrodes. Analytical performance was very good in particular with the electrode GC/Nf/Fe(tm)$_3^{2+}$. The present method can be applied to determine the concentration of nitrite and arsenite in water samples and isoniazid in pharmaceutical formulations. A simple way to tune the hydrophobicity is proposed based on catalyst structure. In future, "hydrophobicity tuning" may be beneficial for a wider range of electrocatalytic processes. The exact nature of the hydrophobicity effect on charge and analyte transport as well as on the analyte - catalyst interaction will require further investigation.

Acknowledgements

UPA acknowledges Council of Scientific and Industrial Research (CSIR), New Delhi for the Senior Research Fellowship. CSIR (01(2708)/13/EMR-II) and University Grants Commission (F 42-271/2013 (SR)), New Delhi are acknowledged gratefully for partial financial support in the form of research projects to VG.

References

1 O. Enea, D. Duprez and R. Amadelli, *Catalysis Today*, 1995, **25**, 271-276.

2 S.E. Andria, C.J. Seliskar and W.R. Heineman, *Anal. Chem*., 2010, **82**, 1720-1726.

3 T-Y. Chen and J. Leddy, *Langmuir,* 2000, **16**, 2866-2871.

4 C.R. Martin, I. Rubinstein and A.J. Bard, *J. Am. Chem. Soc*., 1982, **104**, 4817-4824.

5 D.A. Buttry and F.C. Anson, *J. Am. Chem. Soc*., 1983, **105**, 685-689.

6 A. Moghieb, M.C. Correia and L. McElwee-White, *Inorg. Chim. Acta*, 2011, **369**, 159-164.

7 J. Li, S.J. Guo, Y.M. Zhai and E.K. Wang, *Anal. Chim. Acta,* 2009, **649**, 196-201.

8 T.A. Davis, J.D. Pletcher, D. Genders, Ion Permeable Membranes, The Electrochemical Consultancy Hants, UK, 1997.

9 J. Leddy, Nanomaterials for Sustainable Energy, J.L. Liu, S. Bashir (eds.) in *ACS Symposium Ser*. 2015, **1213**, 99-133.

10 E.V. Milsom, J. Novak, S.J. Green, X.H. Zhang, S.J. Stott, R.J. Mortimer, K. Edler and F. Marken, *J. Solid State Electrochem*., 2007, **11**, 1109-1117.

11 Y. Park, S. Kim, I.H. Jang, Y.S. Nam, H. Hong, D. Choi and W.G. Lee, *Analyst*, 2016, **141**, 1294-1300.

12 U.P. Azad and V. Ganesan, *Chem. Commun*., 2010, **46**, 6156-6158.

13 K.J. Oberbroeckling, D.C. Dunwoody, S.D. Minteer and J. Leddy, *Anal. Chem*., 2002, **74**, 4794-4799.

14 G.V. Zhutaeva, M.R. Tarasevich, M.V. Radina and I.S. Chernyshova, *Russ. J. Electrochem.*, 2009, **45**, 1080-1088.

15 O. Buriez, L.M. Moretto, P. Ugo, *Electrochim. Acta*, 2006, **52**, 958-964.

16 M.S. Faber and S. Jin, *Energy Environ. Sci.*, 2014, **7**, 3519-3542.

17 W.T. Hong, M. Risch, K.A. Stoerzinger, A. Grimaud, J. Suntivich and Y. Shao-Horn, *Energy Environ. Sci.*, 2015, **8**, 1404-1427.

18 H. Dau and I. Zaharieva, *Acc. Chem. Res.*, 2009, **42**, 1861-1870.

19 A. Le Goff, M. Holzinger and S. Cosnier, *Cell. Molecular Life Sci*., 2015, **72**, 941-952.

20 C.N. Shi and F.C. Anson, *Inorg. Chem.*, 1995, **34**, 4554-4561.

21 K. Calfuman, M.J. Aguirre, P. Canete-Rosales, S. Bollo, R. Llusar and M. Isaacs, *Electrochim. Acta,* 2011, **56**, 8484-8491.

22 U.P. Azad, N. Prajapati and V. Ganesan, *Bioelectrochem.*, 2015, **101**, 120-125.

23 J. Madan, A.K. Dwivedi and S. Singh, *Anal. Chim. Acta,* 2005, **538**, 345-353.

24 N. Spataru, T.N. Rao, D.A. Tryk and A. Fujishima, *J. Electrochem. Soc*., 2001, **148**, E112-E117.

25 N.P. Thompson, M.E. Caplin, M.I. Hamilton, S.H. Gillespie, S.W. Clarke, A.K. Burroughs and N. McIntyre, *Eur. Respir. J*., 1995, **8** 1384-1388.

26 A. Salimi, M.E. Hyde, C.E. Banks and R.G. Compton, *Analyst,* 2004, **129**, 9-14.

27 M.H. Pournaghi-Azar and H. Dastangoo, *J. Electroanal. Chem*., 2004, **567**, 211-218.

28 R.K. Hanajiri, R.S. Martin and S.M. Lunte, *Anal. Chem*., 2002, **74**, 6370-6377.

29 J. Liu, W. Zhou, T. You, L. Fenglei, E. Wang and S. Dong, *Anal. Chem*., 1996, **68**, 3350-3353.

30 A.A. Grabinski, *Anal. Chem*., 1981, **53**, 966-968.

31 M.K. Sengupta, M.F. Sawalha, S.I. Ohira, A.D Idowu and P.K. Dasgupta, *Anal. Chem*., 2010, **82**, 3467-3473.

32 Z.H. Wen and T.F. Kang, *Talanta,* 2004, **62**, 351-355.

33 B. Strehlitz, B. Grundig, W. Schumacher, P.M.H. Kroneck, K.D. Vorlop and H. Kotte, *Anal. Chem*., 1996, **68**, 807-816.

34 M.R. Majidi, A. Jouyban and K.*J.* Asadpour-Zeynali, *J. Electroanal. Chem*., 2006, **589**, 32-37.

35 G. Yang, C. Wang, R. Zhang, C. Wang, Q. Qu and X. Hu, *Bioelectrochem.,* 2008, **73**, 37-52.

36 Z-N. Gao, X-X. Han, H-Q. Yao, B. Liang and W-Y. Liu, *Anal. Bioanal. Chem*., 2006, **385**, 1324-1329.

37 S. Sanllorente-Mendez, O. Dominguez-Renedo and M.J. Arcos-Martinez, *Electroanalysis,* 2009, **21**, 635-639.

38 K.B. Male, S. Hrapovic, J.M. Santini and J.H.T. Luong, *Anal. Chem*., 2007, **79**, 7831-7837.

39 U.P. Azad and V. Ganesan, *ChemElectroChem,* 2014, **1**, 279-383.

40 U.P. Azad, S. Turllapati, P.K. Rastogi and V. Ganesan, *Electrochim. Acta,* 2014, **127**, 193-199.

41 C.M. Moore, N.L. Akers, A.D. Hill, Z.C. Johnson and S.D. Minteer, *Biomacromol.,* 2004, **5**, 1241-1247.

42 H.S. White, J. Leddy and A.J. Bard, *J. Am, Chem. Soc*., 1982, **104**, 4811-4817.

43 L.A. Zook and J. Leddy, *Anal. Chem*., 1996, **68**, 3793-3796.

44 U.P. Azad and V. Ganesan, *Electrochim. Acta,* 2011, **56**, 5766-5770.

45 M.G. Almeida, C.M. Silveira and J.J.G. Moura, *Biosens. Bioelectron*., 2007, **22**, 2485-2492.

46 V. Ganesan, S.A. John and R. Ramaraj, *J. Electroanal. Chem*., 2001, **502**, 167-173.

47 U.P. Azad and V. Ganesan, *J. Solid State Electrochem*., 2012, **16**, 2907-2911.

48 J. Burgess and R.H. Prince, *J. Chem. Soc*., 1965, 6061-6066.

49 E. Kubota and M. Yokoi, *Bull. Chem. Soc. Jpn*., 1976, **49**, 2674-2678.

50 M.H. Ford-Smit and N. Sutin, *J. Am. Chem. Soc*., 1961, **83**, 1830-1834.

51 J.N. Richardson, A.L. Dyer, M.L. Stegemiller, I. Zudans, C.J. Seliskar and W.R. Heineman, *Anal. Chem*., 2002, **74**, 3330-3335.

52 S-M. Chen, *Inorg. Chim. Acta,* 1996, **249**, 143-150.

53 A.J. Bard, L.R. Faulkner, *Electrochemical Methods - Fundamentals and Applications*, Wiley, New York, 1980.

54 M. Yagi and T. Sato, *J. Phys. Chem. B*, 2003, **107**, 4975–4981.

55 P. Bertoncello, I. Ciani, F. Li and P.R. Unwin, *Langmuir*, 2006, **22**, 10380–10388.

56 N. Pantelic, C.M. Wansapura, W.R. Heineman and C.J. Seliskar, *J. Phys. Chem. B,* 2005, **109**, 13971-13979.

57 E. Laviron and L. Roullier, *J. Electroanal. Chem.*, 1985, **186**, 1-15.

58 W.J. Albery and A.R. Hillman, *J. Electroanal. Chem*., 1984, **170**, 27-33.

59 W.J. Albery and A.R. Hillman, *Annu. Rep. Prog. Chem., Sect. C: Phys. Chem*., 1981,**78**, 377-437.

60 W. Po, Z. Maia, Z. Daia, Y .Li and X. Zoua, *Biosens. Bioelectron*, 2009, **24**, 3242-3247.

61 P. Kalimuthu and S.A. John, *Electrochem. Commun*., 2009, **11**, 1065-1068.

62 L. Jiang, R. Wang, X. Li, L. Jiang and G. Lu, *Electrochem. Commun*., 2005, **7**, 597-601.

63 Y. Cui, C. Yang, W. Zeng, M. Oyama, W. Pu and J. Zhang, *Anal. Sci*., 2007, **23**, 1421-1425.

64 N. Zhu, Q. Xu, S. Li and H. Gao, *Electrochem. Commun*., 2009, **11**, 2308-2311.

65 W.J.R. Santos, P.R. Lima, A.A. Tanaka, S.M.C.N. Tanaka and L.T. Kubota, *Food Chem*., 2009, **113**, 1206-1211.

66 T-S. Liu, T-F. Kang, L-P. Lu, Y. Zhang and S-Y. Cheng, *J. Electroanal. Chem*., 2009, **632**, 197-200.

67 W.J.R. Santos, A.L. Sousa, R.C.S. Luz, F.S. Damos, L.T. Kubota, A.A. Tanaka and S.M.C.N. Tanaka, *Talanta,* 2006, **70**, 588-594.

68 X. Zhu and X. Lin, *Anal. Sci*., 2007, **23**, 981-985.

69 K. Zhao, H, Song, S, Zhuang, L. Dai, P. He and Y. Fang, *Electrochem. Commun*., 2007, **9**, 65-70.

70 B.R. Kozub, N.V. Rees and R.G. Compton, *Sens. Actuators B,* 2010, **143**, 539-546.